COVER SHEET

NOTE: This coversheet is intended for you to list your article title and author(s) name only —this page will not appear on the CD-ROM.

Paper Number: **477**

Title: **Multiscale Modeling of Carbon Fiber Reinforced Polymer (CFRP) for Integrated Computational Materials Engineering Process**

Authors (names are for example only): Jiaying Gao
Biao Liang
Weizhao Zhang
Zeliang Liu
Puikei Cheng
Ramin Bostanabad
Jian Cao
Wei Chen
Wing Kam Liu
Xuming Su
Danielle Zeng
John Zhao

<<All text below on this page can be deleted >>

PAPER DEADLINE: **June 16, 2017**

PAPER LENGTH: **6-16 PAGES (Maximum – not counting cover page) **

SUBMISSION PROCEDURE: Information on the electronic submission of manuscripts is provided on the conference web site **https://cdmhub.org/groups/asc2017**

FILE NAME: PaperNo_LastName(1st author).doc Example: 1500_Deraco.doc

Please be sure to read these Guidelines prior to preparing your paper—this will ensure your paper is consistent with the format of the articles in the CD-ROM.

NOTE: Please submit your paper in Microsoft Word® format or, if prepared via software other than MSWord, submit as PDF file. Sample guidelines are shown with the correct margins. Follow the style from these guidelines for your page format.

PDF file submission: When making your final PDF for submission make sure the box at "Printed Optimized PDF" is checked. Also—in Distiller—make certain all fonts are embedded in the document before creating the final PDF.

(FIRST PAGE OF ARTICLE – *align this to the top of page – leave space blank above ABSTRACT*)

ABSTRACT

In this work, a multiscale modeling framework for CFRP is introduced to study hierarchical structure of CFRP. Four distinct scales are defined: nanoscale, microscale, mesoscale, and macroscale. Information at lower scales can be passed to higher scale, which is beneficial for studying effect of constituents on macroscale part's mechanical property. This bottom-up modeling approach enables better understanding of CFRP from finest details. Current study focuses on microscale and mesoscale.

Representative volume element is used at microscale and mesoscale to model material's properties. At microscale, unidirection CFRP (UD) RVE is used to study properties of UD. The UD RVE can be modeled with different volumetric fraction to encounter non-uniform fiber distribution in CFRP part. Such consideration is important in modeling uncertainties at microscale level. Currently, we identified volumetric fraction as the only uncertainty parameters in UD RVE. To measure effective material properties of UD RVE, periodic boundary conditions (PBC) are applied to UD RVE to ensure convergence of obtained properties.

Properties of UD is directly used at mesoscale woven RVE modeling, where each yarn is assumed to have same properties as UD. Within woven RVE, there can be many potential uncertainties parameters to consider for a physical modeling of CFRP. Currently, we will consider fiber misalignment within yarn and angle between wrap and weft yarns. PBC is applied to woven RVE to calculate its effective material properties. The effect of uncertainties are investigated quantitatively by Gaussian process.

Preliminary results of UD and Woven study are analyzed for efficacy of the RVE modeling. This work is considered as the foundation for future multiscale modeling framework development for ICME project.

Jiaying Gao, Biao Liang, Weizhao Zhang, Zeliang Liu, Puikei Cheng, Ramin Bostanabad, Jian Cao, Wei Chen, Wing Kam Liu, Department of Mechanical Engineering, Northwestern University, 2145 Sheridan Rd, Evanston, IL 60208-3111, U.S.A.
Xuming Su, Danielle Zeng, Ford Motor Company, Dearborn, MI

John Zhao, LSTC, 7374 Las Positas Road, Livermore, CA 94551

1. INTRODUCTION

Integrated computational material engineering (ICME) for carbon fiber reinforced polymer (CFRP) composite is to develop a simulation tool to predict CFRP's mechanical properties via virtual experiments, such as finite element analysis. This will enable fast development of CFRP by providing vast computational iterations on various CFRP structures and materials. Experimental cost can be reduced due to iterations are conducted over computational frame. The core component of ICME development is multiscale modeling of CFRP. This work requires precise definition of different scales of the material and should provide a streamlined information flow in order to: 1) Top-down, information from upper scale provides modeling parameters for lower scale, which allows lower scale to be different across the higher scale model (i.e., an easy way to interpret it is to image a model with N macroscale material integration points that contain N microscale models); 2) Bottom-up, response of lower scale model under given constraint from higher scale provides precise material response at higher scale.

The hierarchical nature of CFRP makes it a fabulous material for multiscale modeling. The idea behind multiscale modeling for CFRP can be concisely given as: to establish an understanding of CFRP material based on its basic constituents. For CFRP part made of woven CFRP, it can be broken down to different lower scales when macroscale is CFRP part: Mesoscale (woven RVE), Microscale (UD RVE), and Nanoscale. This idea is similar to the effort made in multiscale modeling polymer nanocomposite [1]. For the scale given above, they can be easily integrated based on aforementioned hierarchy since information from lower scales can be easily passed to higher scale [2].

In this work, mesoscale and microscale modeling will be demonstrated. A common approach to model lower scales is to use representative volume element (RVE) that is representative enough of the given microstructure [3]. To ensure imposed overall strain is uniformly distributed within RVE, periodic boundary condition is applied [4]. Another benefit of using Periodic Boundary Condition (PBC) is that using a small RVE will have a good convergence and saves computational time. Therefore, for both woven and unidirectional CFRP (UD), RVEs will be generated using fiber volumetric fraction data measured directly from experiments and PBC will be applied. RVEs at different scales will be used to study material behaviors at that scale and homogenized material properties will be compared to experimental measured values.

In classical homogenization, it assumes all the macro-material points has the same micro-structure, however, for composites, it has found there exists large variation for the microstructure, which is induced by the manufacturing process. In our work, when performing the homogenization, the local inhomogeneity of micro-structure would be accounted. Some microstructure-related parameters are identified and added to characterize the woven RVE structure except the general parameters (like yarn geometry shape and yarn space), which are fiber misalignment within fiber tow, local fiber volume, and variation of yarn angle between warp and weft yarn directions. When such variation exists, woven RVE would have different behavior compared to RVE with perfect fiber alignment and orthotropic warp and weft yarns. To account for such variation, uncertainty quantification is used to quantify its impact. Variation at lower scale will cause different material behavior at higher scale. Multiscale modeling -pro

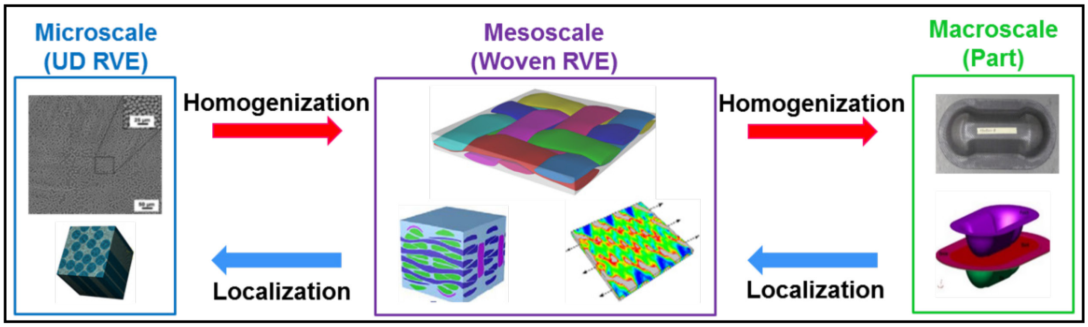

Figure. 1 Schematic of Three-scale Coupling of CFRP in Multiscale Modeling

-vides direct observation of such information pass and effect of uncertainties at higher scales. The multiscale information pass is demonstrated in Figure. 1. In Figure. 1, from macroscale to microscale localization passes microstructure information to RVEs. In contrast, homogenization passes stress and material constitutive laws from microscale to macroscale.

2. MICROSCALE UD RVE MODELING

The microscale study focuses on UD RVE modeling. The UD properties is approximated using UD RVE through hominization. Equivalent material properties are compared to experimental measurements. If the model is validated by experimental values then the UD RVE can be used to calculate mechanical properties of UD with different microstructure, such as UD with different fiber volumetric fraction.

2.1. Definition of UD RVE

UD is defined as CFRP that contains fibers only in one direction. Fibers are assumed to be perfectly straight although wavy fiber might be observed in certain cases [6]. Here both fiber and resin properties are known and fiber distribution is assumed to be random according to experimental observation shown in Figure. 2. A UD RVE can be simply defined as UD structure with limited number of fibers within a given domain. When the domain is fixed, altering number of fibers will result in different volumetric fraction V_f.

Ideally the ICME process will intake digital image of UD sample as RVE, but currently resolution of UD image is rather low. Thus, artificial UD RVE with circular fiber and random distribution is generated by algorithm developed at NU. UD RVE is generated with voxel mesh elements with random fiber distribution. Different volumetric fraction can be generated easily by adding more fibers within the domain. Here, voxel mesh is performed over conforming mesh due to following reasons:1) Voxel mesh is easy to generate and has good compatibility with current automated pre/post processing scripts; 2) Image based UD RVE generated from digital image will naturally be voxel format because the voxel is the basic element of an image. By being consistent with voxel mesh format the UD RVE can be easily switched to image based. By defining local stress tensor at each integration point within RVE as $\boldsymbol{\sigma}^{micro}$, the homogenized stress $\overline{\boldsymbol{\sigma}}$ in the RVE is defined as:

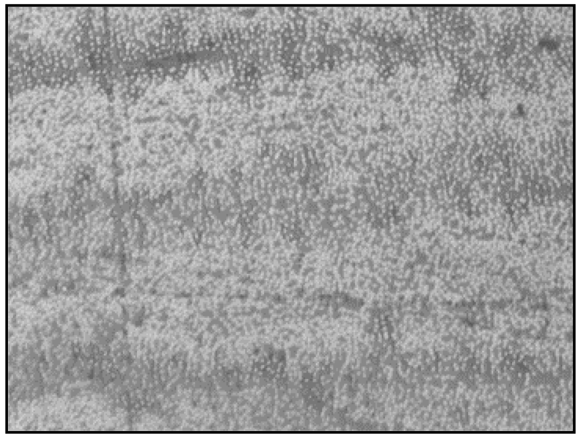

Figure. 2 CT Image of UD with Average V_f = 51% and Random Fiber Distribution

$$\bar{\boldsymbol{\sigma}} = \frac{1}{|V|}\int_V \boldsymbol{\sigma}^{\mathrm{micro}}\, dV \tag{1}$$

Where V is the RVE domain

In a similar fashion, local strain tensor $\boldsymbol{\varepsilon}^{micro}$ leads to homogenized strain $\bar{\boldsymbol{\varepsilon}}$ in the RVE as:

$$\bar{\boldsymbol{\varepsilon}} = \frac{1}{|V|}\int_V \boldsymbol{\varepsilon}^{\mathrm{micro}}\, dV \tag{2}$$

Once the homogenization procedure is completed, stress and strain tensors for each RVE will be available to compute equivalent material properties of UD. The relationship between $\bar{\boldsymbol{\sigma}}$ and $\bar{\boldsymbol{\varepsilon}}$ is:

$$\bar{\boldsymbol{\sigma}} = \boldsymbol{C}:\bar{\boldsymbol{\varepsilon}}$$

Where C is the effective stiffness tensor of the RVE.

2.2. UD RVE Simulation

The UD study serves three major purposes:1) To quantitatively measure UD properties and validate against experimental measurement; 2) Utilize UD RVE to observe its response under tension or shear loading conditions; 3) Extract UD response as constitutive law for upper level mesoscale model, where each integration point on yarn will intake UD response instead of pre-assigned material constants.

The UD RVE assumes no damage or imperfection. Volumetric fraction of fiber V_f is fixed within single RVE simulation, but V_f can be a random value. Fiber is considered as elastic material and resin matrix is considered as elastic-plastic material with J2 plasticity law calibrated to resin test. Hardening law is assumed in exponential form, shown below:

$$\sigma_Y = -a_2 \exp(-a_1 \varepsilon_{eq}^{pl}) + a_3 \tag{3}$$

Where σ_Y is the yield stress and ε_p is equivalent plastic strain. Exponential law parameters are chosen as a1 = 185 MPa, a2 = 85 MPa, and a3 = 111 MPa based on the available experimental results of matrix material.

As stated in section 2.1, homogenized stress and strain can be calculated easily for given RVE. Write strain and stress tensors in Voigt notation and use compliance matrix **S** to express linear elastic material model when plasticity is not considered:

$$\begin{bmatrix} \varepsilon_{11} \\ \varepsilon_{22} \\ \varepsilon_{33} \\ \gamma_{12} \\ \gamma_{13} \\ \gamma_{23} \end{bmatrix} = \begin{bmatrix} s_{11} & s_{12} & s_{13} & s_{14} & 0 & 0 \\ & s_{22} & s_{23} & s_{24} & 0 & 0 \\ & & s_{33} & s_{34} & 0 & 0 \\ & & & s_{44} & 0 & 0 \\ & symmetry & & & s_{55} & s_{56} \\ & & & & & s_{66} \end{bmatrix} \begin{bmatrix} \sigma_{11} \\ \sigma_{22} \\ \sigma_{33} \\ \sigma_{12} \\ \sigma_{13} \\ \sigma_{23} \end{bmatrix} = [\mathbf{S}]_{1-2-3} \begin{bmatrix} \sigma_{11} \\ \sigma_{22} \\ \sigma_{33} \\ \sigma_{12} \\ \sigma_{13} \\ \sigma_{23} \end{bmatrix}$$

(4)

Note here the compliance matrix **S** is given as a general form for monoclinic material, meaning 13 constants needs to be calculated. UD is a special form of monoclinic material, transverse isotropic. Therefore, it will have zeros for S_{14}, S_{24}, S_{34} and S_{56}, leaving total of 9 constants to be calculated. To compute each component of **S**, it is convenient to introduce stress-free state, meaning each loading only introduce one of the stress tensor **σ** to have a significant larger magnitude comparing to other five will be negligible due to difference in magnitude. However, in each stress-free state all six strain components will not be zero. Using above matrix, each column of **S** can be computed easily. By introducing periodic boundary condition (PBC), the UD RVE can represent UD CFRP material and six stress-free state loading simulations can be done to obtain effective material properties of UD CFRP.

The UD RVE of V_f =51% constructed is shown in Figure. 3 below, with mesh resolution of 300 x 300 in 2-3 plane to ensure accurate capture of fiber shape. Following observation made over experimental image shown in Figure. *2*, fibers are randomly distributed and in circular shape. Fiber and matrix material constants are given in TABLE. I. Material direction is given as: 1 for fiber direction, 2 and 3 for transverse direction where 1 is orthogonal to plane 2-3. Six loading cases are studied with macroscopic strain of 3.5% applied to 11, 22, 33, 12, 13, and 23 directions.

Equivalent elastic material constants are computed and compared against experimental value to validate the simulation. Shown in Figure. 4 below. Good match in Young's moduli, G_{23} and poison's ratios are observed. G_{12} and G_{23} from RVE homogenization are smaller than smallest value observed from experiments. Such inconsistency might be caused by difference in fiber geometry between UD RVE and UD sample used in experiments.

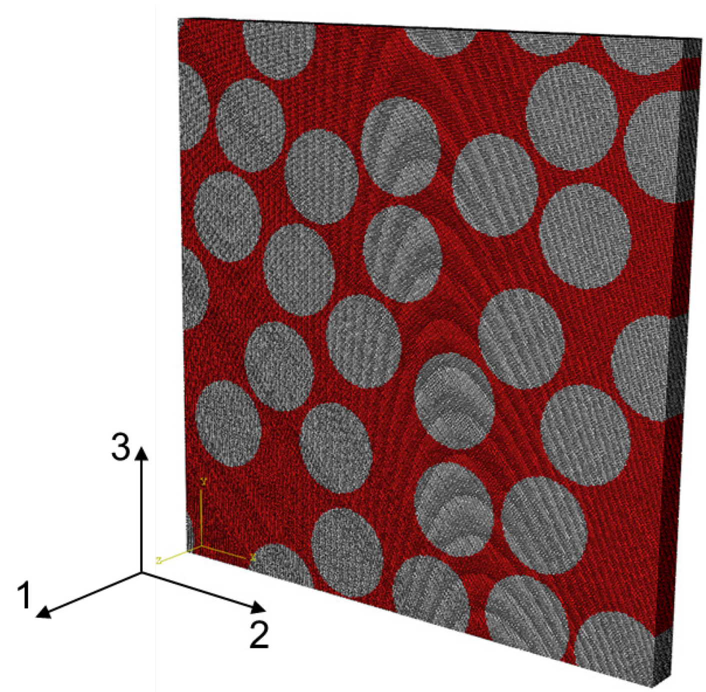

Figure. 3 UD RVE Voxel Mesh with Circular Fiber with Random Fiber Distribution

.

TABLE. I FIBER AND MATRIX PROPERTIES OF CURED WOVEN

Fiber	E_{11}	E_{22}	E_{33}	G_{12}	G_{13}	G_{23}	ν_{12}	ν_{13}	ν_{23}
	245 GPA	19.8 GPA	19.8 GPA	29.2 GPA	29.2 GPA	5.92 GPA	0.28	0.28	0.671

Matrix	E	ν
	3.79 GPA	0.39

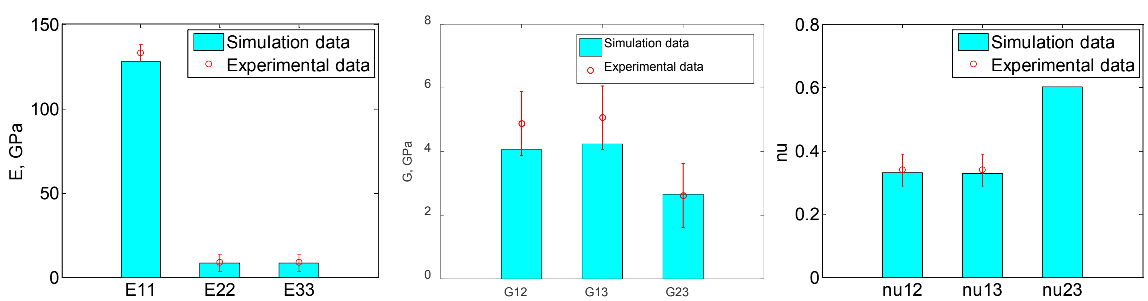

a) Young's Moduli b) Shear Moduli c) Poisson's Ratio

Figure. 4 UD Elastic Material Constants: RVE Homogenized vs. Experimental Measurements: a) Young's Moduli; b) Shear Moduli; c) Poisson's Ratio

Stress and strain curves obtained from longitudinal and transverse tension simulations are shown in Figure. 5 and compared against experimental values. The figures reveal good consistency in initial elastic regions but divergence are observed in plastic region before UD sample reach failure in experiment. A possible explanation for such inconsistence is fibers in simulation are assumed to be perfect elastic. Plasticity is

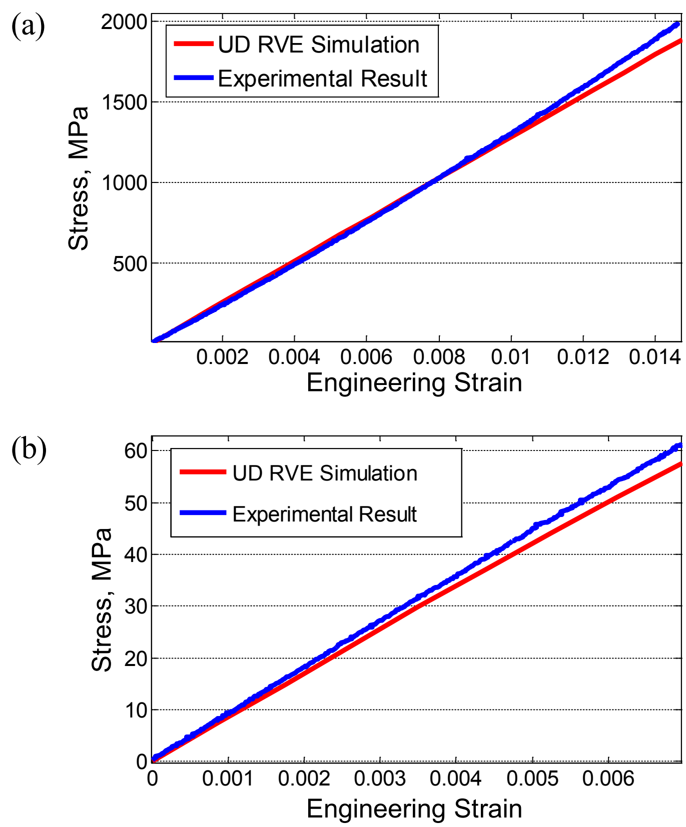

Figure. 5 Stress and Strain Curves for RVE DNS and Experimental Measurement under (a) Longitudinal and (b) Transverse Tension Loadings

only considered in matrix. If fiber undergo any unexpected non-linear behavior the simulation might diverge from experimental measurements. Another potential cause of disagreement is the matrix plasticity. Current matrix plasticity only calibrated to tension test. However, the yielding surface of matrix might not be a von Mise type, but more like a Drucker-Prager type. More experiments will be conducted to reveal difference in matrix property under tension and compression. Pressure-dependency will be considered for matrix in future work.

The UD RVE simulations shown good match with experimental results. The results shown are for UD with 51% volumetric fraction but cases with other volumetric fraction are also done. However, no uncertainty parameters are considered in modeling process. In the future, the UD RVE modeling will incorporate potential imperfection introduced in manufacturing process to make a better representation of real material. Moreover, material model will be further calibrated to reduce difference between simulation and experimental results. The UD RVE properties are incorporated in woven RVE simulation, as will be introduced in next section.

3. Mesoscale Cured Woven Modeling

For CFRP part made with woven composite, mesoscale modeling of woven is necessary to connect microscale to macroscale, as illustrated in Figure. 6. Each macroscale element in the part shall call woven RVE and pass ε^{macro} to it. This will result in strain filed across woven RVE. At mesoscale level, constitutive equation of resin is provided but not for yarn. Each element in yarn will call microscale UD RVE using specific microstructure information such as volumetric fraction or fiber misalignment. UD RVE will then feedback constitutive information back to yarn for calculation of stress. Finally, woven RVE will pass σ^{macro} to macroscale model. Homogenization between woven RVE and macroscale part is same as shown in Section 2.1. In this work, woven is twill woven. Uncertainties can be introduced in woven RVE modeling to study the effect of possible imperfection introduced during manufacturing process of woven, such as non-orthogonal woven and fiber misalignment within each yarn.

3.1. Definition of Woven and RVE Size Selection and PBC

By definition given in [7], minimum repeating unit of twill consists of four warp and four weft yarn and it is used as woven RVE. Here the woven we choose is 2x2 twill woven. The 2x2 woven geometry shown in Figure. 7 is designed to satisfy overall fiber volume fraction 51 % in woven， which is calculate as product of volumetric fraction V_y of all yarns within woven RVE and V_f of fiber within each yarn (same in all yarns).

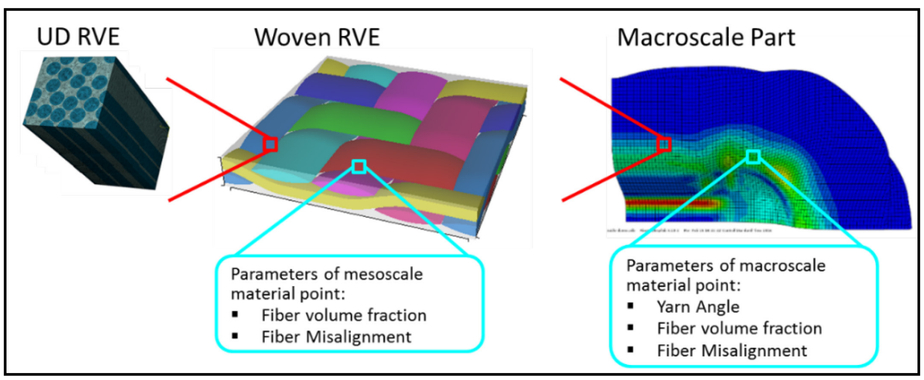

Figure. 6 Information Pass for CFRP Three-scale Model

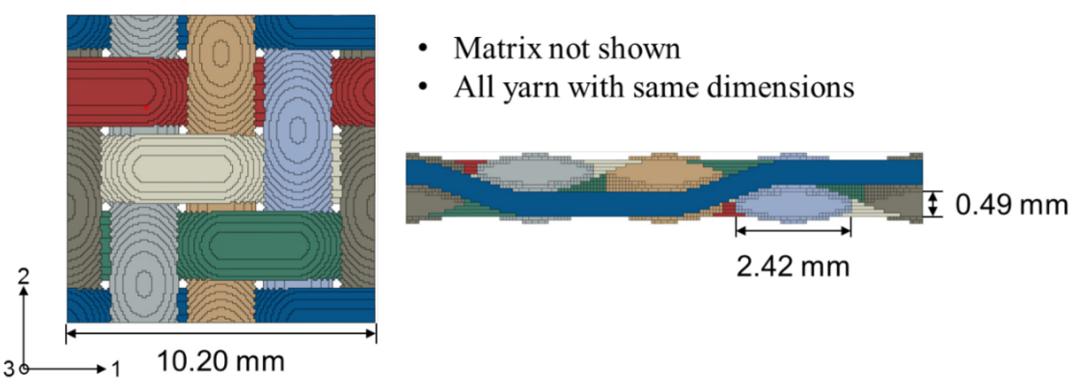

Figure. 7 Woven RVE Dimensions

Model is generated by TenGen [8] and woven RVE has eight yarns in total, where all yarns are assumed to have same properties.

3.2. Woven RVE Simulation

Woven RVE study is currently elastic analysis to provide elastic constants of woven CFRP. Yarn properties are based on homogenization results of UD RVE introduced in previous section to link microscale RVE to mesoscale RVE.

By calculating compliance matrix **S** of woven RVE, stiffness matrix **C** can be found easily. **C** provides a direct observation of woven properties. This will assist the following uncertainty analysis, accompanied by preliminary results.

3.3. Uncertainty and Preliminary Results

To explore the effect of uncertainty in woven RVE, the woven RVE with uncertainties can be modeled to observe change in overall homogenized material due to variation in microstructure. Three uncertainty parameters are considered in this study: 1. Fiber misalignment within the yarn; 2. Yarn angle between warp and weft yarns; 3. Random volumetric fraction distribution within woven. Those uncertainty parameters distinguish our work from other study on woven RVE because traditional homogenization study of woven RVE treats all above parameters as constants. By including uncertainty parameters the multiscale model is able to account for different variation in microstructure observed in actual part and provides more accurate prediction on mechanical properties. In this section, the focus in on mesoscale woven RVE and see how woven properties are affected by random volumetric distribution and fiber misalignment.

For each material point in woven RVE, it is possible to assign different V_f (represents V_f of fibers within each yarn) and fiber misalignment parameters to investigate effect of both on overall mechanical properties. The volumetric fraction at each material point can modified by assigning different V_f and mechanical properties are then assigned according to UD with same V_f.

Same operation can be done for fiber misalignment. The fiber misalignment is considered as the deviation from perfect alignment direction. Shown in Figure. 8, vector $\vec{\mathbf{g}}_1$ represents direction of perfect fiber direction, which is essentially the tangent line of yarn center line. Plane $\vec{\mathbf{g}}_2\vec{\mathbf{g}}_3$ is the yarn cross-section and $\vec{\mathbf{g}}_1$ is orthogonal to the plane.

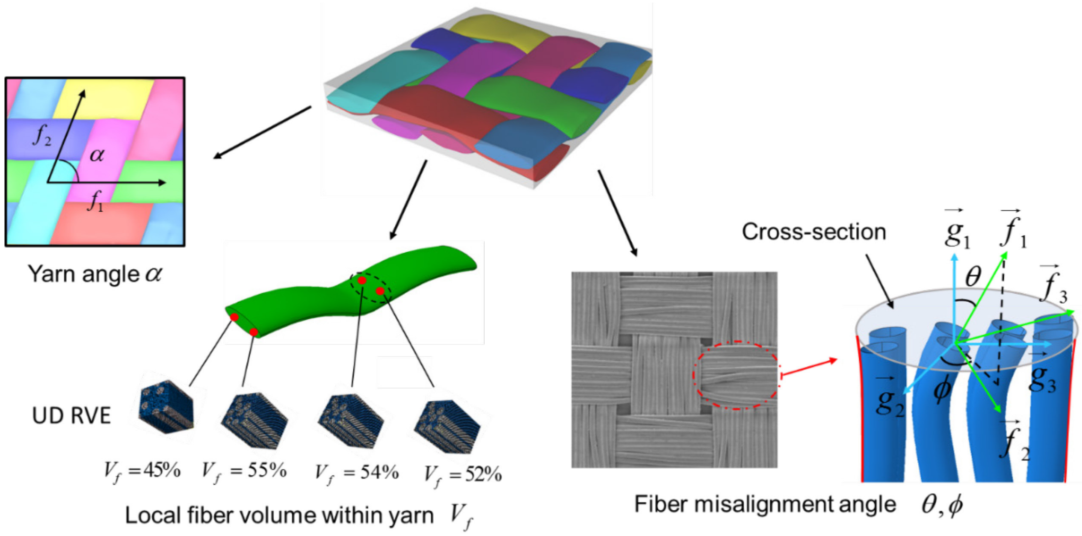

Figure. 8 Schematic of different uncertainty parameters considered for Woven RVE

Angle θ (0º ≤ θ ≤ 90º) and Φ (-180º ≤ Φ ≤ 180º) are used to establish misaligned fiber direction $\vec{\mathbf{f}}_1$. $\vec{\mathbf{f}}_1$, $\vec{\mathbf{f}}_2$, and $\vec{\mathbf{f}}_3$ represent transverse isotropic material frame accounting for fiber misalignment. Equations for calculating $\vec{\mathbf{f}}_1$, $\vec{\mathbf{f}}_2$, and $\vec{\mathbf{f}}_3$ given as below:

$$\begin{cases} \vec{f}_1 = \frac{\vec{g}_2}{\|\vec{g}_2\|}\sin\theta\cos\Phi + \frac{\vec{g}_3}{\|\vec{g}_3\|}\sin\theta\sin\Phi + \frac{\vec{g}_1}{\|\vec{g}_1\|}\cos\theta \\ \vec{f}_2 = \frac{\vec{g}_2}{\|\vec{g}_2\|}\cos\theta\cos\Phi + \frac{\vec{g}_3}{\|\vec{g}_3\|}\cos\theta\sin\Phi - \frac{\vec{g}_1}{\|\vec{g}_1\|}\sin\theta \\ \vec{f}_3 = \vec{f}_1 \times \vec{f}_2 \end{cases} \tag{5}$$

In order to consider aforementioned uncertainties in woven RVE, Gaussian distribution is assumed for these parameters. V_f follows Gaussian distribution by letting mean $\overline{V}_f$ = 65% and variance $\sigma^2_{V_f}$ = 0.09%. For fiber misalignment, θ and Φ follow Gaussian distribution by letting mean $\overline{\theta} = 10°$, variance $\sigma^2_\theta = 2$, mean $\overline{\Phi} = 0°$, and variance $\sigma^2_\Phi = 2500°^2$ (to make sure for all element within yarn, its Φ will fall between -180º and 180º following three sigma rule). For each yarn, V_f follows Gaussian distribution. All yarns are assumed to have same distribution function. 30 realizations are done for V_f. Doing same for θ & Φ by assigning θ & Φ following Gaussian distribution to all material points with 30 realizations.

In Figure. 9, histogram of E_{11} for woven with Gaussian distribution of V_f in Gaussian distribution is plotted. The distribution of E_{11} follows Gaussian distribution, as expected. Moreover, TABLE. II shows percentage difference of homogenized material properties between constant V_f and V_f in Gaussian distribution. The difference is small, but the Von Mises stress contour of in-plane shear deformation in Figure. 10 shows locally the two models have different behaviors. Such variation in Von Mises stress contour demonstrates the effect of V_f in local stress distribution. The no-fiber-misalignment vs. fiber-misalignment tells the same story. TABLE. III shows with misalignment woven RVE has considerate difference in E_{11}, E_{22} and E_{12}. All those directions are fiber dominant direction and when fibers are misaligned the strength should change accordingly. From Von Mises stress contour of in-plane shear deformation shown in Figure. 11, it is clear that fiber-misalignment causes huge variation in Von Mises stress contour and higher maximum stress in woven RVE. Above observations are enough to show the importance of uncertainty in woven RVE modeling. More trials will be carried out in future work, including design-of-experiment, to fully understand effect of uncertainties in woven RVE modeling.

The woven RVE study indicates that microstructure change due to uncertainty will impact mechanical properties. Therefore the multiscale framework should consider such variation to truthfully represent real material.

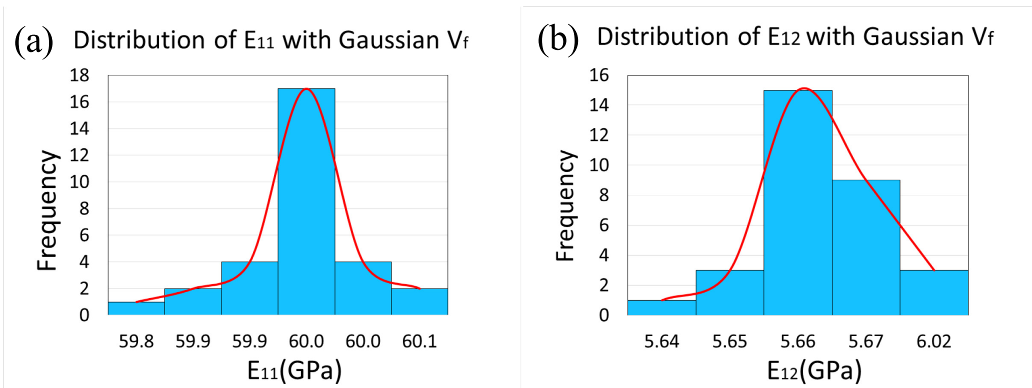

Figure. 9 Distribution of (a) E_{11} and (b) E_{12} with V_f in Woven RVE Following Gaussian Distribution

TABLE. II EFFECT OF VF ON HOMOGENIZED MATERIAL PROPERTIES

	E_{11} (GPa)	**E_{22} (GPa)**	**E_{33} (GPa)**	**E_{12} (GPa)**	**E_{13} (GPa)**	**E_{23} (GPa)**
V_f= 65%	59.96	59.96	12.57	5.68	3.60	3.60
$\bar{V}_f$= 65%, $\sigma^2_{V_f}$ = 0.09%	59.96	59.94	12.60	5.66	3.58	3.58
Percentage Difference (%)	**0.0011**	**0.0218**	**0.2128**	**0.4066**	**0.4436**	**0.4425**

TABLE. III EFFECT OF FIBER MISALIGNMENT ON HOMOGENIZED MATERIAL PROPERTIES

	E_{11} (GPa)	**E_{22} (GPa)**	**E_{33} (GPa)**	**E_{12} (GPa)**	**E_{13} (GPa)**	**E_{23} (GPa)**
No-Misalignment	59.96	59.96	12.57	5.68	3.60	3.60
$\bar{\theta}$ = 10°, σ^2_θ = 2 $\bar{\Phi}$ = 0°,σ^2_Φ = 2500	48.01	47.14	12.42	6.15	3.67	3.68
Percentage Difference (%)	**24.89**	**27.19**	**1.17**	**7.69**	**1.88**	**2.15**

a) Constant V_f Woven RVE b) Gaussian Distributed V_f Woven RVE

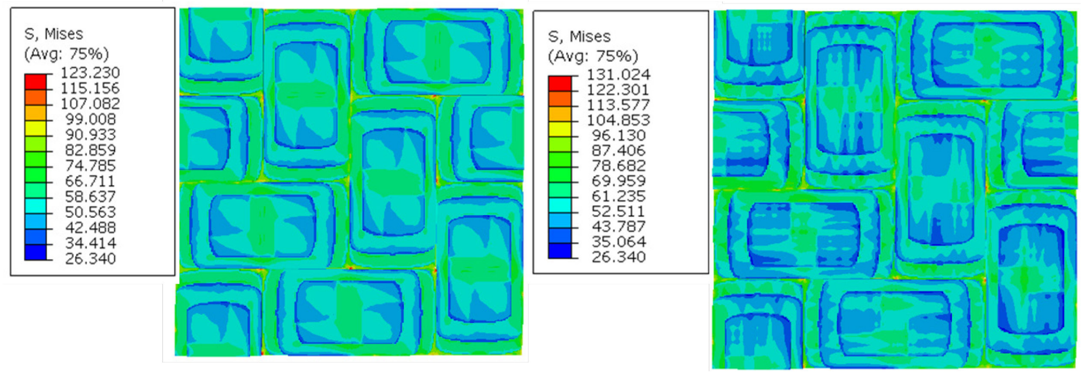

Figure. 10 Von Mises Stress Plot of woven with (a) constant V_f and (b) Gaussian distributed V_f under in-plane shear deformation

a) Woven RVE without Fiber Misalignment b) Woven RVE with Fiber Misalignment

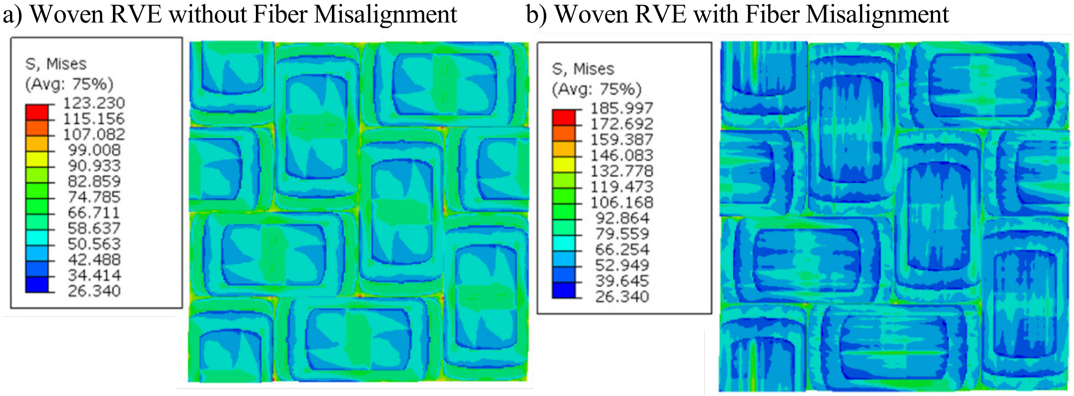

Figure. 11 Von Mises Stress Plot of (a) woven without fiber misalignment (b) woven with fiber misalignment under in-plane shear deformation

4. Future work and Conclusion

In this work, microscale and mesoscale modeling of CFRP in a multiscale simulation framework has been introduced. Preliminary results of UD RVE are in good match with experimental observation. For woven RVE, the effective woven properties under different uncertainty parameters are discussed and the results reveal that such uncertainty is not to be neglected.

The results obtained in this work also demonstrated impact of microstructure in multiscale modeling for CFRP. For ICME development, it will benefit from multiscale simulation framework with microstructure information integrated in the whole work flow. By further exploring the cause of uncertainty, it is possible to link manufacturing parameters to change in microstructure in CFRP.

Acknowledgements

The authors thank financial support through a subcontract from the Ford Motor Company with funding from the U.S. Department of Energy's Office of Energy Efficiency and Renewable Energy (EERE), under Award Number DE-EE0006867.

REFERENCES

1. Li, Ying, Shan Tang, Brendan C. Abberton, Martin Kröger, Craig Burkhart, Bing Jiang, George J. Papakonstantopoulos, Mike Poldneff, and Wing Kam Liu. "A predictive multiscale computational framework for viscoelastic properties of linear polymers." Polymer 53, no. 25 (2012): 5935-5952.
2. Melro, A. R., P. P. Camanho, FM Andrade Pires, and S. T. Pinho. "Numerical simulation of the non-linear deformation of 5-harness satin weaves." Computational Materials Science 61 (2012): 116-126.
3. Kanit, T., S. Forest, Ia Galliet, Va Mounoury, and D. Jeulin. "Determination of the size of the representative volume element for random composites: statistical and numerical approach." International Journal of solids and structures 40, no. 13 (2003): 3647-3679.
4. Li, Shuguang, and Anchana Wongsto. "Unit cells for micromechanical analyses of particle-reinforced composites." Mechanics of materials 36, no. 7 (2004): 543-572.
5. Feyel, Frédéric. "A multilevel finite element method (FE 2) to describe the response of highly non-linear structures using generalized continua." Computer Methods in applied Mechanics and engineering 192, no. 28 (2003): 3233-3244.
6. Joyce, Peter J., Danielle Kugler, and Tess J. Moon. "A technique for characterizing process-induced fiber waviness in unidirectional composite laminates-using optical microscopy." Journal of composite materials 31, no. 17 (1997): 1694-1727.
7. Oelsner, Gustaf Hermann. A handbook of weaves. Macmillan Company, 1915.
8. Long, A. C., and L. P. Brown. "Modelling the geometry of textile reinforcements for composites: TexGen." Composite reinforcements for optimum performance. Cambridge: Woodhead Publishing Ltd (2011): 239-64.
9. Daniel, Isaac M., Ori Ishai, Issac M. Daniel, and Ishai Daniel. Engineering mechanics of composite materials. Vol. 3. New York: Oxford university press, 1994.